Biaxial Orientation Induced in a Photoaddressable Azopolymer Thin Film As Evidenced by Polarized UV−Visible, Infrared, and Raman Spectra

T. Buffeteau,[†] F. Lagugné Labarthet,[†] C. Sourisseau,*[†] S. Kostromine,[‡] and T. Bieringer[‡]

Laboratoire de Physico-Chimie Moléculaire (UMR 5803-CNRS), Université Bordeaux 1, 351 cours de la Libération, 33 405 Talence Cédex, France, and Central Research Department, Bayer AG, D-51368 Leverkusen, Germany

Received September 8, 2003

ABSTRACT: The main goal of this spectroscopic study was to obtain relevant information about the symmetry properties for a thin film of a new class of photoaddressable azopolymers, which are known to display a huge birefringence (Δn exceeding −0.45 at 632.8 nm) and a high stability and are attractive materials for rewritable recording media and optical memories. First, various real-time birefringence experiments are performed using a linearly polarized irradiation at 532.0 nm and probing the thin film sample at 675.0 nm to confirm the largest Δn values ever reported for such amorphous polymers. Then, polarized transmission measurements in the UV−visible and mid-infrared spectral ranges are compared for an isotropic and anisotropic sample. They provide strong evidences for cooperative orientational effects and for the establishment of a biaxial symmetry; the two average orientation factors $\langle F_{2,0}\rangle$ and $\langle F_{2,2}\rangle$ are thus extracted from infrared data for several vibrational modes. The remaining and related fourth rank factors, namely $\langle F_{4,0}\rangle$, $\langle F_{4,2}\rangle$ and $\langle F_{4,4}\rangle$, are then determined from the confocal micro-Raman spectra recorded under various polarization configurations, more precisely from the two Raman intensity ratios, $R_1 = I_{XY}/I_{XX}$ and $R_2 = I_{YX}/I_{YY}$. Reasonable values of the different orientation order parameters are thus obtained allowing to determine the overall orientation distribution function of the chromophores, in particular for the ω(C═C) ring (8a) vibrational mode at 1599 cm^{-1}. Definitive conclusions are thus drawn about the effective biaxial symmetry in this copolymer sample.

Introduction

In the past few years, azobenzene-containing polymer systems have been the subject of intensive research because of their potential uses in photonics, optoelectronics, and optical signal processing.[1−3] In particular, they have attracted much interest for rewritable recording media due to the reversible transformation of their molecular orientation upon irradiation with a linearly polarized light; the key mechanism is due to the photoisomerization cycles of the trans and cis isomers of azobenzenes, which drive the major axis of the molecules in the direction perpendicular to the light polarization and lead to the appearance of strongly anisotropic properties.[4−6] In this respect, large birefringence values connected to this reorientation process were reached and extensively investigated for use in real-time holography.[7−11]

Generally, the molecular orientation in these systems is deducted from a simple model in which it is assumed that the orientation distribution of the azobenzene units with respect to the radiation polarization direction is uniaxial. However, the uniaxial model is not necessarily valid for materials exhibiting a large birefringence. Indeed, a photoinduced biaxiality has already been observed by Wiesner et al.[12,13] on liquid-crystalline copolymers containing cyanoazobenzene and cyanophenylbenzoate groups in side-chain positions, in which the mesogens are preferentially aligned normal to the film plane; in that case, a cooperative motion of the photoactive (cyanoazobenzene) and nonphotoactive (cyanophenylbenzoate) side chains is of significant importance in the establishment of biaxiality. In contrast, most copolymers in which the azobenzene groups are statistically copolymerized with methyl methacrylate display a very low biaxiality. More recently, Buffeteau and Pézolet[4] have characterized a photoinduced biaxiality in thin films of a disperse red19 containing semicrystalline azopolymer (pDR19t) with phenylene diacrylate groups in the main chain. When pDR19t films are irradiated with a polarized laser, the azobenzene groups reorient perpendicularly to the direction of the laser polarization with a preferred orientation inside the film plane; in this infrared study, cooperative motions of the azobenzene and phenylene units were evidenced. From the above examples, it appears that cooperative motions in azopolymers increase the birefringence of the material, but they may induce a biaxial orientation of the chromophores. In this respect, an interesting new class of photoaddressable polymers (hereafter called PAP) has recently been synthesized in the Bayer laboratories.[5,14] For instance, in the family of K1−*x* copolymers the material contains in side-chain positions two functional groups: first, chromophores of azobenzene derivatives (*x*%) used as antenna for the incident light, and, second, mesogenic side groups ((1−*x*)%) leading to the possible existence of an intermediate liquid-crystalline mesophase. The task of the mesogenic side groups is to follow the light-induced reorientation of the chromophores, to stabilize and amplify the new chromophore configuration. As a matter of fact, a large birefringence value of −0.23 at 632.8 nm has been observed in a K1−

* To whom correspondence should be addressed. E-mail: c.sourisseau@lpcm.u-bordeaux1.fr.
[†] Université Bordeaux 1.
[‡] Bayer AG.

10.1021/ma030471g CCC: $27.50
Published on Web 03/20/2004

Chart 1. Chemical Formula of the PAP1−50 Photoaddressable Copolymer

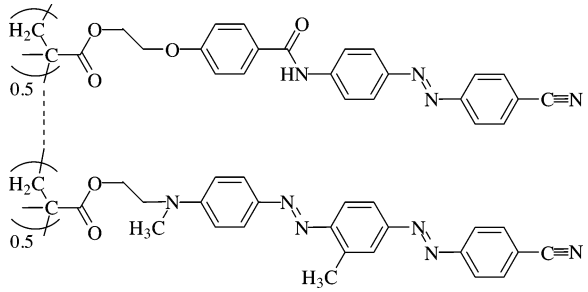

30 thin film (30% azo content) after irradiation and biaxial properties were evidenced by waveguide light mode measurements. Similar effects, in particular enhancements in a cooperative alignment, are also expected to take place in the PAP1−*x* system under study (hereafter called PAP1−50 sample, see Chart 1), which contains not only a cyano-substituted diazobenzene part (*x*%), but also another mesogenic cyanoazobenzene part; here, both side groups are present in equal amounts (50%) and are able to serve as light absorbing centers. However, as far as we know, the optical and symmetry properties of such a strongly absorbing material have not yet been extensively investigated.

In this study we have thus focused our attention on polarization measurements in UV−visible, FTIR and Raman spectroscopies, which are able to indicate any deviation from a simple uniaxial symmetry in polymer thin films. From the data treatments, we have further characterized the extent of biaxiality created upon a laser beam irradiation and calculated the values of the five average orientation factors characteristic of the biaxial system.

This paper is thus organized as follows: In the next section, the material and experimental setup are described. In the theoretical part, the expressions of the order parameters involved in uniaxial and biaxial systems and of the related orientation distribution functions are recalled, in connection with their possible estimates from FTIR and Raman experiments on a polymer thin film. Then, in the results section the UV−visible, FTIR, and micro-Raman spectra recorded under various polarization geometries are presented, and in the following discussion part, the more probable values of the effective orientation factors are calculated. This allows us to draw conclusions about the nature of biaxiality in the PAP1−50 polymer system and to establish the form of the distribution function for a characteristic ω(C═C) vibrational ring mode of the chromophores.

Experimental Section

Materials. As shown in Chart 1, the PAP1−50 copolymer exhibits a unique structure containing equal amounts of azomesogenic (top) and diazo-chromophoric (below) side chains chemically attached via $(CH_2)_2$ units to a polymethacrylate (PMMA) polymer backbone.[14,15] This amorphous copolymer has a glass transition temperature of 114 °C (DSC, 20 K/min) and the following values of average molecular weight: Mn = 4600, M_w = 20 000 and D = M_w/M_n = 4.35 (GPC method using PMMA calibration in dimethylacetamide at 40 °C). As compared with the series of previously prepared K1−*x* related copolymers,[5,16,17] both side chains display now a similar dimension and contain a cyano group only in the "para" position maximizing the electronic delocalization; therefore, the electronic absorption bands in the visible region will be very intense and, again, the band of the diazo-monomer unit will be shifted to the longer wavelength side (≈500 nm) with respect to the azo-mesogenic part (≈350 nm), so that each azobenzene chromophore would play a photoactive part, depending on the wavelength of the actinic light.

Thin films of the PAP1−50 sample were prepared by spin-coating from THF solutions onto glass or NaCl flat optical windows, and their thicknesses were in the 375−420 nm range. Such red-brown films are strongly colored.

Experimental Measurements. In situ dynamic measurements of the induced linear birefringence were performed on a homemade instrument, inserting the sample between two crossed linear polarizers and using a photoelastic modulator with a CaF_2 crystal (Hinds PEM80) just before the sample. A diode laser at 675 nm was used as a light probe and optical anisotropy was induced in the copolymer film with the help of a linearly polarized laser at 532 nm (CrystaLaser).[9] Additional measurements were also performed using the 632.8 and 820.0 nm probing laser lines.

Unpolarized (on the isotropic starting films) and polarized (on the films after a laser writing) UV−visible absorption spectra (300−900 nm) were recorded on a Safas DES instrument in the transmission mode. Similarly, polarized infrared spectra were recorded, before and after the irradiation, with a Nicolet NEXUS 670 FTIR interferometer. The absorbances parallel ($A_{||}$ or A_X) and perpendicular ($A_\perp$ or A_Y) to the laser polarization were measured using a wire grid BaF_2 polarizer (Specac) mounted in front of the sample. The absorbance A_Z was calculated by subtracting the A_X and A_Y values from the mean absorbance, $A_0 = (A_X + A_Y + A_Z)/3$, obtained for the starting sample assumed to be isotropic; the initial nearly isotropic property was previously checked from 45° incidence transmission measurements in the visible region.

To avoid strong absorption effects and fluorescence phenomena, the Raman spectra have been recorded using the 752.5 nm line of a mixed Kr−Ar laser with a very weak incident intensity on the sample (0.1−0.2 mW) and a Labram (from Jobin-Yvon, Horiba group, France) Raman confocal microspectrometer. A wide-angle 100× (numerical aperture NA = 0.90) objective lens was used in conjunction with a relatively large confocal aperture (≈500 μm) and a typical acquisition time of 30 s; under such preresonance Raman conditions, the spectra exhibited a good signal-to-noise ratio. The intensity and polarization calibrations of our microscope optical setup were checked using the responses of the isotropic initial sample. For the polarized Raman measurements, the polarization direction of the incident beam was intentionally kept fixed, but the scattered light was analyzed using a vertical or horizontal analyzer in conjunction with a polarization scrambler located in front of the entrance slit. Moreover, as shown in Figure 1, two series of such experiments were performed before and after a 90° rotation of the sample under the microscope stage, i.e., with the incident electric field either parallel (Figure 1a) or perpendicular (Figure 1b) to the pump beam writing direction; this direction was always along the *X* axis. Therefore, as discussed below, the values of the two following Raman intensity ratios $R_1 = I_{XY}/I_{XX}$ and $R_2 = I_{YX}/I_{YY}$ have been experimentally determined, allowing one to obtain estimates of the orientation factors for any vibrational mode.

Theoretical Part: Main Order Parameters in Uniaxial and Biaxial Systems and Related Orientation Distribution Functions

Uniaxial Systems. The forms of the orientational distribution functions for probe molecules of cylindrical symmetry embedded in uniaxial centrosymmetric systems have already been largely considered from the second-rank and fourth-rank Legendre polynomials, $\langle P_l(\cos\theta)\rangle$ order parameter values. In particular, from the knowledge of both the $\langle P_2\rangle$ and $\langle P_4\rangle$ parameters the distribution function $f(\theta)$, which is completely defined by the polar angle θ between the unique long symmetry

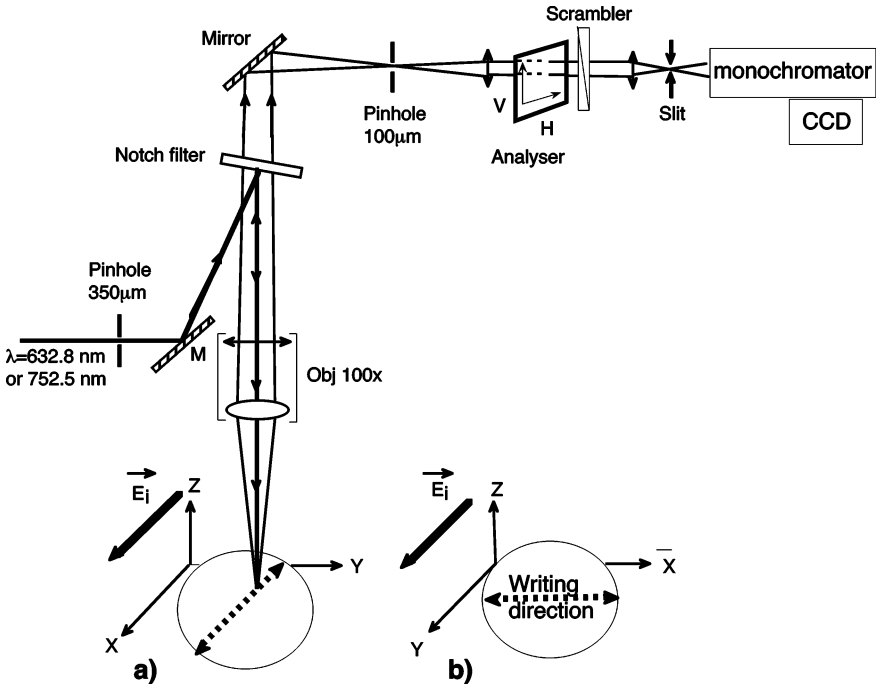

Figure 1. Experimental setup for recording the polarized micro-Raman experiments: (a) measurements of the *XX* and *XY* spectra in the first configuration; (b) measurements of the *YY* and *YX* spectra in the second configuration.

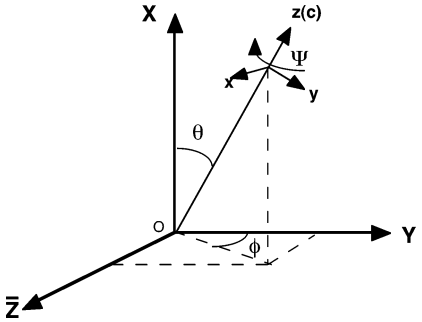

Figure 2. Definition of the θ, Φ, and Ψ Euler angles in the laboratory coordinate system and of the *x*, *y*, and *z* axes of the molecular system.

axis of the chromophore and a local laboratory vertical axis as shown in Figure 2, may be expanded in terms of Legendre polynomials in cos(θ) as follows:

$$f(\theta) = \sum_{l=0}^{4}{}^{\text{even}}\left(1 + \frac{1}{2}\right)\langle P_l\rangle\, P_l(\cos\,\theta) \qquad (1)$$

where

$$\langle P_0(\cos\,\theta)\rangle = 1.0$$

$$\langle P_2(\cos\,\theta)\rangle = \frac{1}{2}(3\langle\cos^2\theta\rangle - 1)$$

$$\langle P_4(\cos\,\theta)\rangle = \frac{1}{8}(35\langle\cos^4\theta\rangle - 30\langle\cos^2\theta\rangle + 3) \qquad (2)$$

Generally, $\langle P_2\rangle$ values are determined from UV−visible or FTIR measurements; meanwhile, both $\langle P_2\rangle$ and $\langle P_4\rangle$ values can be reached for instance from Raman or fluorescence polarized data and/or from NMR studies. However, these spectroscopic techniques cannot provide the complete distribution of orientation but give only a limited number of "orientation averages", and finally, the series expansion of eq 1 is not always converging. Under these conditions, according to Berne et al.[18] and following the arguments of Pottel et al.,[19] one may estimate the most probable equilibrium function by using the powerful information entropy theory. Introducing the Lagrange multipliers λ_2 and λ_4, the following expression of the most probable and normalized distribution function $f_{\text{mp}}(\theta)$ is derived:

$$f_{\text{mp}}(\theta) = \frac{\exp[\lambda_2 P_2(\cos\,\theta) + \lambda_4 P_4(\cos\,\theta)]}{\int_0^\pi \exp[\lambda_2 P_2(\cos\,\theta) + \lambda_4 P_4(\cos\,\theta)]\,\sin\,\theta d\theta} \qquad (3)$$

Moreover, for uniaxial systems centered perpendicularly to any constraint direction, i.e., behaving as a negative $\langle P_2\rangle$ value within the 0.0 to −0.5 range, we have recently demonstrated that four distinct domains can be distinguished in the ($\langle P_2\rangle$, $\langle P_4\rangle$) half-plane, and they lead to different typical shapes of the $f_{\text{mp}}(\theta)$ functions.[20] More precisely, for any $\langle P_2\rangle$ value and increasing $\langle P_4\rangle$ ones, we encounter a first domain of unimodal asymmetric functions, a second domain of Gaussian distributions (centered at 90°) and two successive domains of bimodal asymmetric shape functions.

Biaxial Systems. In such systems the projection of any transition moment may be considered unevenly distributed within the (*Y*, *Z*) plane (Figure 2), but because of the "fiber symmetry" of the rodlike chromophores, one may assume a random rotation about the third Ψ Euler angle. For such a biaxial distribution of orientations, the generalized orientation factors $F_{l,m}$ have been reported by Nomura et al.[21] and by Jarvis et al.[22] for normalized and nonnormalized Legendre polynomials, respectively. The two set of coefficients differ slightly, except the $F_{l,0}$ factors which are identical to those above-defined ($\langle P_2\rangle$, $\langle P_4\rangle$) in uniaxial "fiber symmetry" systems.[23] According to Nomura et al.[21] we thus arrive at the following average expressions

$$\langle F_{2,0}\rangle = \langle P_2(\cos\theta)\rangle = \frac{1}{2}(3\langle\cos^2\theta\rangle - 1) = f_\theta$$

$$\langle F_{4,0}\rangle = \langle P_4(\cos\theta)\rangle = \frac{1}{8}(35\langle\cos^4\theta\rangle - 30\langle\cos^2\theta\rangle + 3) \quad (4)$$

and

$$\langle F_{2,2}\rangle = 12\langle P_{2,2}(\cos\theta)\rangle = 3\langle\sin^2\theta.\cos2\phi\rangle = 2f_\phi(1 - f_\theta)$$

$$\langle F_{4,2}\rangle = 180\langle P_{4,2}(\cos\theta)\rangle = \frac{15}{2}\langle(-7\cos^4\theta + 8\cos^2\theta - 1).\cos2\phi\rangle$$

$$\langle F_{4,4}\rangle = 1680\langle P_{4,4}(\cos\theta)\rangle = 105\langle\sin^4\theta\cos4\phi\rangle \quad (5)$$

Note that for the f_θ and f_Φ functions we have also made use of the Kaito et al. notation,[24] which is very convenient and is of practical use in FTIR measurements:

$$f_\theta = \frac{1}{2}(3\langle\cos^2\theta\rangle - 1)$$

$$f_\Phi = \frac{\langle\sin^2\theta\cos2\phi\rangle}{\langle\sin^2\theta\rangle} \quad (6)$$

Indeed, following the axis definitions in Figure 2, the various polarized absorbance FTIR components are

$$A_X \approx \langle\cos^2\theta\rangle = A_0(2f_\theta + 1)$$

$$A_Y \approx \langle\cos^2\phi\,\sin^2\theta\rangle = A_0(1 - f_\theta)(1 + f_\Phi)$$

$$A_Z \approx \langle\sin^2\phi\,\sin^2\theta\rangle = A_0(1 - f_\theta)(1 - f_\Phi) \quad (7)$$

where A_0 is the mean absorbance, i.e.

$$A_0 = (A_X + A_Y + A_Z)/3 \quad (8)$$

Therefore, assuming that the mean absorbance does not change upon irradiation, to determine the f_θ and f_Φ functions under consideration it will be sufficient to perform a first measurement on the initial isotropic polymer film and, then, two experiments on the same anisotropic sample using the polarization along the *X* and *Y* directions, respectively:

$$f_\theta(\text{biax}) = \frac{(A_X/A_0) - 1}{2} = \frac{A_X - \left(\frac{A_Y + A_Z}{2}\right)}{(A_X + A_Y + A_Z)}$$

$$f_\phi(\text{biax}) = \frac{(A_Y - A_Z)}{(A_Y + A_Z)} \quad (9)$$

We may easily verify that for an isotropic sample $f_\theta = f_\Phi = 0.0$; meanwhile, for an homogeneous uniaxial system with the long molecular axes along the *X* direction, one must find $f_\theta = 1.0$ and $f_\Phi = 0.0$. In contrast, for the cases of perfect biaxial symmetry with a complete orientation either along the *Y* direction (in the film plane) or in the *Z* direction (perpendicular to the film plane), we expect $f_\theta = -0.5$ in both cases and f_Φ equal to +1.0 or −1.0, respectively.

The problem is obviously more complex when dealing with Raman results since the Raman scattering data in a biaxial system are sensitive to all the five $F_{l,m}$ factors already defined in eqs 4 and 5. Experimentally, only two ratios of polarized relative Raman intensities can be determined using a linearly polarized incident laser beam and, several important intensity corrections are necessary when working on a confocal microscope instrument with a wide angle objective lens.[25,26]

Actually, in the theoretical treatment of the intensities in micro-Raman spectroscopy one must take into consideration the nature of the incident and scattered electric fields and carry out a double integration over the total scattering volume (*V*) and the solid angle of collection (Ω):[25−29]

$$I_{IJ} \cong \int_V\int_\Omega (|E_{\text{inc}}\alpha_{IJ}E_{\text{scat}}|^2)\,\mathrm{d}\mathbf{\Omega}\,\mathrm{d}V \quad (10)$$

In polarization analyses with an anisotropic sample, considering only the first more important terms dependent on the C_0 component of the energy distribution of the incident field, we arrive at the following simple relations:

•For an incident laser beam linearly polarized along the *X* direction (Figure 1a) one expects

$$I_{XY} \cong (A\langle\alpha_{XY}{}^2\rangle + B\langle\alpha_{XZ}{}^2\rangle)[2C_0] + ...$$

$$I_{XX} \cong (A\langle\alpha_{XX}{}^2\rangle + B\langle\alpha_{XZ}{}^2\rangle)[2C_0] + ... \quad (11)$$

•For an incident laser beam linearly polarized along the *Y* direction (Figure 1b), we obtain

$$I_{YX} \cong (A\langle\alpha_{YX}{}^2\rangle + B\langle\alpha_{YZ}{}^2\rangle)[2C_0] + ...$$

$$I_{YY} \cong (A\langle\alpha_{YY}{}^2\rangle + B\langle\alpha_{YZ}{}^2\rangle)[2C_0] + ... \quad (12)$$

Experimentally, we determine the two intensity ratios $R_1 = I_{XY}/I_{XX}$ and $R_2 = I_{YX}/I_{YY}$, respectively, which are thus dependent on the A and B parameters due to the collection efficiency of the scattering, i.e., on the "effective semi-angle of scattering" (θ'_m) within the sample defined by

$$\sin\theta'_m = \frac{1}{n}\sin\theta_m = \frac{NA}{n^2} \quad (13)$$

where NA is the objective lens numerical aperture, $\theta_\mathbf{m}$ and $\theta'_\mathbf{m}$ are the incidence half-angles of the light in air and in the sample of refractive index (*n*). The analytical expressions for *A* and *B* are

$$A = \pi^2\left(\frac{4}{3} - \cos\theta'_m - \frac{1}{3}\cos^3\theta'_m\right)$$

$$B = 2\pi^2\left(\frac{2}{3} - \cos\theta'_m + \frac{1}{3}\cos^3\theta'_m\right) \quad (14)$$

In the present study, we have used a mean refractive index equal to 1.681 (at 752.5 nm)[5,14] leading to $A = 2.841$ and $B = 0.452$, when using a 100× objective lens of NA = 0.90.

Finally, the intensity ratios are also dependent on the orientational average quantities of the polarizability tensor components

$$\langle\alpha_{IJ}{}^2\rangle \approx \int_0^{2\pi}\mathrm{d}\phi\int_{-1}^{+1}\langle\alpha_{IJ}{}^2F_{l,m}(\cos\theta,\phi)\rangle\,\mathrm{d}(\cos\theta) \quad (15)$$

which can be calculated using the "complete" expression (up to the fourth order) of the distribution function in a biaxial system:

$$F(\cos\theta,\phi) = \frac{1}{4\pi^2}\left\{\begin{aligned} &\frac{1}{2} + \frac{5}{4}(3\cos^2\theta - 1)\langle F_{2,0}\rangle \\ &+ \frac{5}{8}(\sin^2\theta\cos 2\phi)\langle F_{2,2}\rangle \\ &+ \frac{9}{16}(35\cos^4\theta - 30\cos^2\theta + 3)\langle F_{4,0}\rangle \\ &- \frac{3}{16}(7\cos^4\theta - 8\cos^2\theta + 1)(\cos 2\phi)\langle F_{4,2}\rangle \\ &+ \frac{3}{128}(\cos^4\theta - 2\cos^2\theta + 1)(\cos 4\phi)\langle F_{4,4}\rangle \end{aligned}\right\} \quad (16)$$

Therefore, we have developed the calculations for the vibrational modes behaving a molecular polarizability tensor of cylindrical symmetry,

$$\begin{pmatrix} \alpha_1 & & \\ & \alpha_1 & \\ & & \alpha_3 \end{pmatrix}$$

in which the α_3 element is largely dominant ($\alpha_3 \gg \alpha_1$) and uses the Euler angles already defined in Figure 2. After simple mathematics we arrive at the following expressions:

• In the first set of experiments with the incident laser beam linearly polarized along the *X* direction (Figure 1a)

$$[\alpha_{XY}] = [(\alpha_3 - \alpha_1)\sin\phi\sin\theta\cos\theta]$$

and, therefore

$$\langle\alpha_{XY}{}^2\rangle \cong \frac{\alpha_3{}^2}{105}\{7 + 5\langle F_{2,0}\rangle - 2.5\langle F_{2,2}\rangle - 12\langle F_{4,0}\rangle - \langle F_{4,2}\rangle\} \quad (17)$$

$$[\alpha_{XZ}] = [(\alpha_3 - \alpha_1)\cos\phi\sin\theta\cos\theta]$$

$$\langle\alpha_{XZ}{}^2\rangle \cong \frac{\alpha_3{}^2}{105}\{7 + 5\langle F_{2,0}\rangle + 2.5\langle F_{2,2}\rangle - 12\langle F_{4,0}\rangle + \langle F_{4,2}\rangle\} \quad (18)$$

$$[\alpha_{XX}] = [\alpha_3\cos^2\theta + \alpha_1\sin^2\theta]$$

$$\langle\alpha_{XX}{}^2\rangle \cong \frac{\alpha_3{}^2}{105}\{21 + 60\langle F_{2,0}\rangle + 24\langle F_{4,0}\rangle\} \quad (19)$$

and this leads to the first intensity ratio R_1 expression:

$$R_1 = [7(A+B) + 5(A+B)\langle F_{2,0}\rangle - 12(A+B)\langle F_{4,0}\rangle - 2.5(A-B)\langle F_{2,2}\rangle - (A-B)\langle F_{4,2}\rangle]/[7(3A+B) + 5(12A+B)\langle F_{2,0}\rangle + 12(2A-B)\langle F_{4,0}\rangle + 2.5(B)\langle F_{2,2}\rangle + (B)\langle F_{4,2}\rangle] \quad (20)$$

•Similarly, in the second set of experiments with the laser beam linearly polarized along the Y direction (Figure 1b) one obtains

$$[\alpha_{YZ}] = [(\alpha_3 - \alpha_1)\sin\phi\cos\phi\sin^2\theta]$$

$$\langle\alpha_{YZ}{}^2\rangle \cong \frac{\alpha_3{}^2}{105}\{7 - 10\langle F_{2,0}\rangle + 3\langle F_{4,0}\rangle - 0.125\langle F_{4,4}\rangle\} \quad (21)$$

$$[\alpha_{YY}] = [(\alpha_3 - \alpha_1)\sin^2\phi\sin^2\theta + \alpha_1]$$

$$\langle\alpha_{YY}{}^2\rangle \cong \frac{\alpha_3{}^2}{105}\{21 - 30\langle F_{2,0}\rangle + 9\langle F_{4,0}\rangle - 15\langle F_{2,2}\rangle + \langle F_{4,2}\rangle + 0.125\langle F_{4,4}\rangle\} \quad (22)$$

so, the second intensity ratio R_2 has the following expression:

$$R_2 = [7(A+B) + 5(A-2B)\langle F_{2,0}\rangle - 3(4A-B)\langle F_{4,0}\rangle - 2.5(A)\langle F_{2,2}\rangle - (A)\langle F_{4,2}\rangle - 0.125(B)\langle F_{4,4}\rangle]/[7(3A+B) - 10(3A+B)\langle F_{2,0}\rangle + 3(3A+B)\langle F_{4,0}\rangle - 15(A)\langle F_{2,2}\rangle + (A)\langle F_{4,2}\rangle + 0.125(A-B)\langle F_{4,4}\rangle] \quad (23)$$

Note that Jarvis et al.[22] have already proposed other similar Raman intensity expressions by making uses of a different laboratory axis system and of the nonnormalized $\langle\mathbf{P}_{l,m}\rangle$ orientation factors, instead of the normalized $\langle\mathbf{F}_{l,m}\rangle$ ones; so, we have checked that all the expressions are consistent and can be nicely compared. More importantly, the above approach shows that the solution of the problem can only be found by a proper combination of infrared and Raman results and by using an additional assumption: from the knowledge of both the $\langle\mathbf{F}_{2,0}\rangle$, $\langle\mathbf{F}_{2,2}\rangle$ factors determined in FTIR and from a sensible value assumed for the $\langle\mathbf{F}_{4,0}\rangle$ parameter, we shall be able to get an estimate of the two remaining order parameters, $\langle\mathbf{F}_{4,2}\rangle$, $\langle\mathbf{F}_{4,4}\rangle$, by considering the R_1 and R_2 experimental ratio values. Therefore, it will be possible to establish the chromophore orientation distribution function corresponding to each vibrational mode from the five distinct orientation coefficients, by using eq 16 in conjunction with a very probable Φ angular value. This will allow us to discuss in details the extent of the biaxiality created in the PAP1−50 system under a polarized beam irradiation.

Results

Birefringence Measurements. Real-time birefringence variations, probed at 675 nm (outside the main absorption bands) for a thin film of 370 nm thickness, upon a 750 s irradiation at 532 nm (irradiance ≈350 mW/cm^2) and upon relaxation during another period of 750 s are shown in Figure 3. In agreement with previous studies on this copolymer and on related compounds[5,14,15,30] we do observe a stable and large birefringence value, equal to −0.342 just before the laser is off and equal to −0.337 at the end of the relaxation period. It is noteworthy that, using another thicker film (417 nm) and a stronger irradiance of 900 mW/cm^2 at 514.5 nm, an even larger birefringence plateau value of −0.496 has been reached when probing the system at 632.8 nm.[31] Due to unique structures of the azo-mesogenic and diazobenzenic chromophore side-chain units chemically linked to the polymer backbone and, probably, to strong cooperative dipolar and steric effects, this PAP1−50 material exhibits, to the best of our

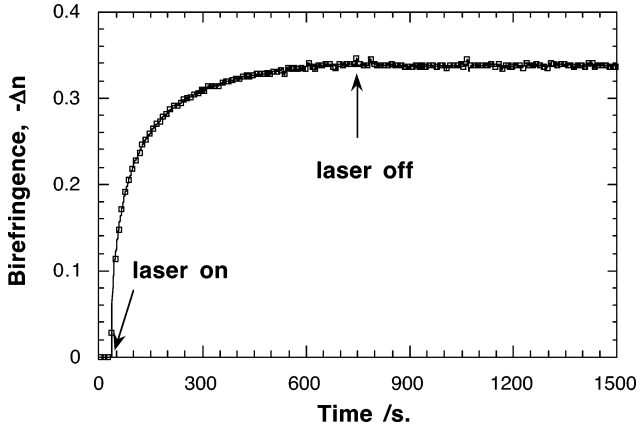

Figure 3. Plot of the real-time linear birefringence inscription during a 750 s period with a pump beam at 532 nm with an irradiance of 350 mW/cm^2 and of the relaxation process during another 750 s period with the pump beam "off".

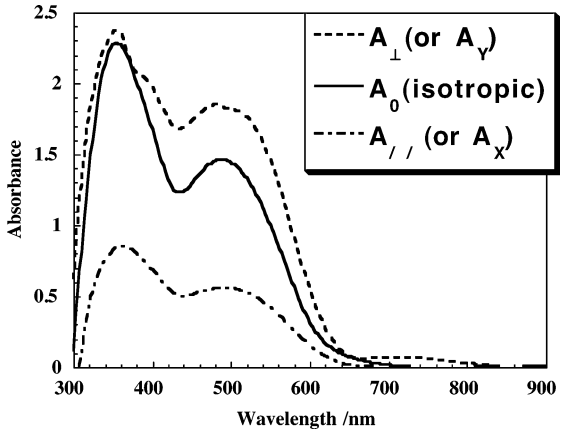

Figure 4. UV−visible absorption spectra of an initially isotropic PAP1−50 thin film (dashed lines) and of the $A_\perp$ (A_Y; full lines) and $A_{||}$ (A_X; dot−dashed lines) polarized responses for the birefringent sample after irradiation with a linearly polarized beam.

knowledge, the largest record Δn values ever reported for a class of such amorphous azopolymers.

UV−Visible Spectroscopy. As shown in Figure 4, the electronic absorption spectrum of an isotropic thin film displays two intense bands maximizing at 490 and 354 nm. By analogy with results obtained for a series of K1−*x* related copolymer compounds,[5,16,17] these bands can be assigned to transitions essentially localized into the diazoic and azo-mesogenic side groups, respectively. Furthermore, after irradiation with a linearly polarized beam, the absorbance along the parallel direction $A_{||}$ (or A_X) exhibits a drastic intensity decrease, whereas the absorbance in the perpendicular direction $A_\perp$ (or A_Y) is slightly increased.

Under the assumption of uniaxial symmetry, the above polarized results allow normally to retrieve the isotropic spectrum using the simple spectral addition, $(A_{||} + 2A_\perp)/3$. In fact, this relation is not perfectly satisfied and, over the 440−700 nm wavelength range, we may only suggest a mean value of the $\langle P_2 \rangle$ order parameter, $\langle P_2 \rangle = (A_{||} - A_\perp)/(A_{||} + 2A_\perp)$, roughly equal to −0.31. We thus conclude to the existence of strong orientational effects and, as expected, the long axis of the chromophores is preferentially orientated in the perpendicular directions. Nevertheless, the uniaxial model is probably a very crude approximation approach and, to check the above conclusions, we have established

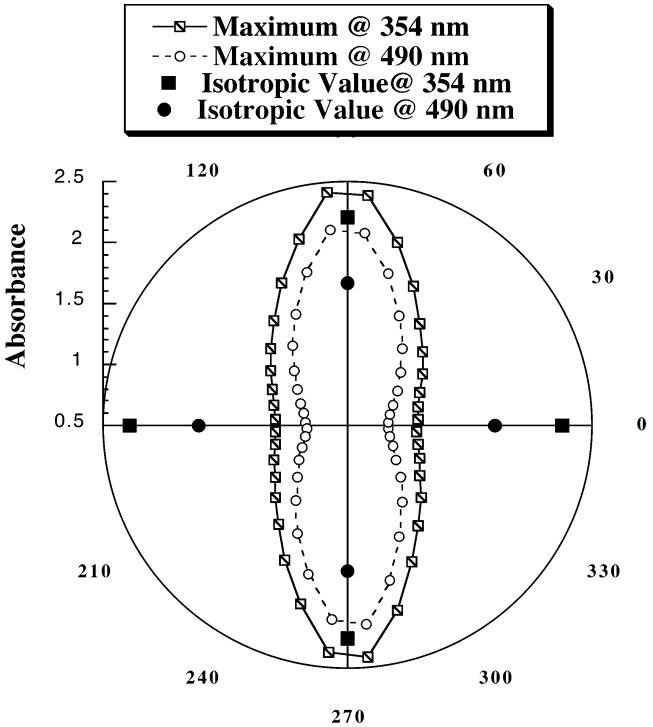

Figure 5. Polar plots of the absorbance variations at the 354 and 490 nm maxima for a birefringent sample; measurements were performed in the transmission mode at normal incidence applying successive 10° rotations in the film plane.

the polar plots of the absorbance variations at the maxima of both electronic bands; for this purpose, we have applied successive 10° rotations to the irradiated film into the spectrometer sample compartment. The results of such measurements are reported in Figure 5, where the electric field of the polarized pumping laser beam is assumed along the horizontal direction (0°). We thus confirm the preferential orientation of both diazo- and azo-mesogen chromophores in a perpendicular direction (90°), but it is hard to explain why the amplitudes and widths of both distributions are so different. Moreover, such results do not allow to rule out definitively the uniaxial symmetry although, under this assumption, a quite large $\langle P_2 \rangle$ value equal to −0.355 would be effective for the band maximum at 490 nm assigned to the diazo-chromophore side-chain.

FTIR Measurements. Infrared band intensities in the 2400−600 cm^{-1} range can be compared on the survey spectrum of the isotropic sample (Figure 6a) and on the polarized spectra of the anisotropic thin film (Figure 6b). Note that the assignments of several characteristic vibrational modes are indicated in Figure 6a and the corresponding absorbance variations are gathered in Table 1. It is noteworthy that strong dichroic effects are observed for many bands and, in a first approximation, the modes ν(C≡N) at 2226 cm^{-1}, ω(C═C) (8a) at 1599 cm^{-1}, 19(a) at 1506 cm^{-1}, ν(N═N) at 1372 cm^{-1}, $\nu_{asym.}$(Φ-N) at 1308 cm^{-1}, δ(CH) (9a) at 1141 cm^{-1} and $\nu_{sym.}$(Φ-N) at 1089 cm^{-1} appear the more polarization sensitive ones; they all correspond to internal vibrations of the diazo- or azo-mesogenic units, whose transition moments are likely orientated along their long molecular axis. In contrast, quite distinct and lower absolute values are observed for the ν(N−H) mode at 3357 cm^{-1} (not shown in Figure 6), ν(O(−C═O)) at 1730 cm^{-1} and ν(N(−C═O)) vibration at 1676 cm^{-1}, with f_θ values equal to −0.079, −0.023, and +0.200, respec-

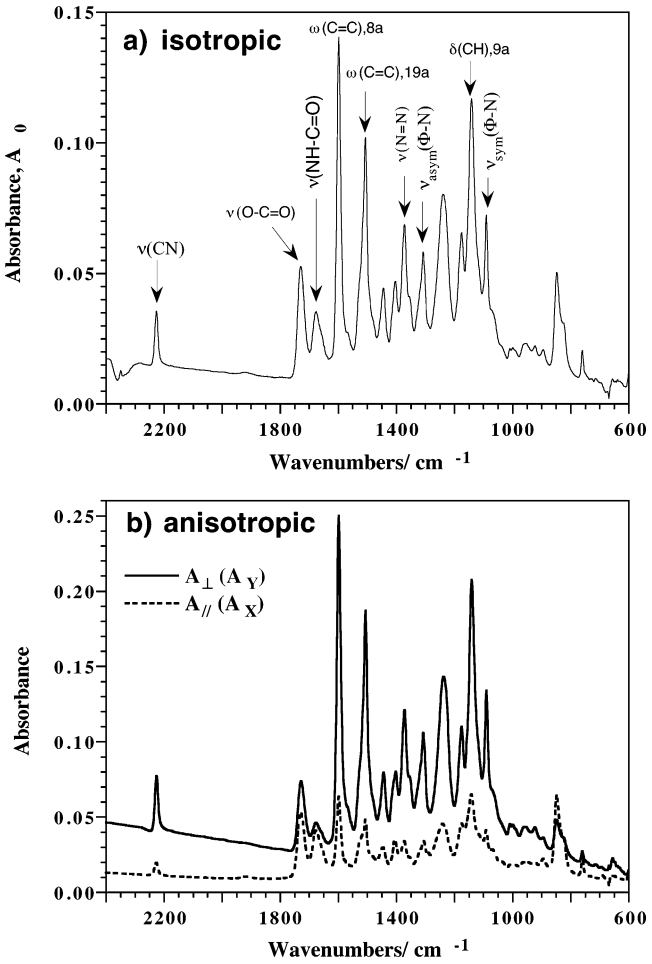

Figure 6. Infrared absorbance spectra in the 2400−600 cm^{-1} range of (a) an initially isotropic PAP1−50 thin film (some band assignments are indicated) and (b) of the $A_\perp$ (A_Y; full line) and $A_{||}$ (A_X; dashed line) polarized responses for the birefringent sample after irradiation with a linearly polarized beam.

Table 1. Main Absorbance Values Observed in FTIR Spectra and Estimates of Both Orientation Functions f_θ and f_ϕ under the Uniaxial and Biaxial Models

ν/cm^{-1}	A_0	$A_X = A_{\|\|}$	$A_Y = A_\perp$	A_Z	f_θ uniax	f_θ biax	f_ϕ biax
3357	0.0035	0.0039	0.0050	0.0016	−0.079	+0.057	+0.515
2226	0.0207	0.0085	0.0373	0.0163	−0.347	**−0.295**	**+0.392**
1730	0.0410	0.0420	0.0450	0.0360	−0.023	+0.012	+0.111
1676	0.0210	0.0280	0.0160	0.0190	+0.200	+0.167	−0.086
1599	0.1230	0.0483	0.2150	0.1057	−0.349	**−0.304**	**+0.341**
1506	0.0800	0.0310	0.1430	0.0660	−0.353	**−0.306**	**+0.368**
1372	0.0420	0.0150	0.0690	0.0420	−0.353	**−0.321**	**+0.243**
1308	0.0300	0.0123	0.0525	0.0252	−0.343	**−0.295**	**+0.351**
1141	0.0900	0.0406	0.1550	0.0744	−0.326	**−0.275**	**+0.351**
1089	0.0480	0.0165	0.0875	0.0400	−0.371	**−0.328**	**+0.372**

tively, but their transition moment is surely not parallel to the chromophore long axis. For the former modes, the strongly negative f_θ values of about −0.349 (±0.013) determined under the uniaxial symmetry assumption are in accordance with previous results from the UV−visible spectra and in agreement with a reorientation in the perpendicular directions. However, as discussed below, this is a very crude approximation since the significant differences observed on the A_Y and A_Z absorbances are a clear indication that a biaxial symmetry has taken place in this anisotropic sample (Table 1).

Micro-Raman Experiments. Polarization analyses of the Raman scattered radiation from an isotropic sample lead to the I(VH) and I(VV) spectra reported in Figure 7, which are also called $I(XX)$ and $I(XY)$ spectra, respectively (see Figure 1a). The good signal-to-noise responses allow us to estimate the depolarization ratio, $I(XY)/I(XX)$, which is nearly equal to 0.33 for most of the chromophore vibrational modes. We thus conclude that the scattering bands are due to totally symmetric vibrations, which are enhanced by preresonance effects involving an uniaxially polarized electronic transition; since the enhanced modes are likely to display a diagonal polarizability tensor of cylindrical symmetry,

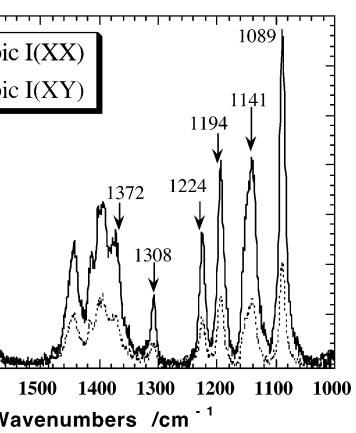

Figure 7. Polarized Raman scattering spectra of an isotropic PAP1−50 thin film in the 1800−1000 cm^{-1} range. The I_{XX} (full lines) and I_{XY} (dashed line) polarized responses are reported, and some band wavenumbers are indicated.

$$\begin{pmatrix} \alpha_1 & & \\ & \alpha_1 & \\ & & \alpha_3 \end{pmatrix}$$

this confirms that the α_3 element is dominant ($\alpha_3 \gg \alpha_1$). Of course, we have assumed that the very weak irradiance of the incident laser beam at 752.5 nm has not perturbed the initial isotropy in the film plane.[32]

Then, for the anisotropic sample we have recorded two series of Raman spectra under various polarization configurations, namely $Z(XX)Z'$ and $Z(XY)Z'$ on one hand, to determine the R_1 intensity ratio, and $Z(YY)Z'$ and $Z(YX)Z'$ on the other hand, to obtain the R_2 ratio; the corresponding spectra in the 1800−1000 cm^{-1} range are reported in Figure 8, parts a and b, respectively. Note that these survey spectra display similar features, but the $I(YY)$ spectrum is markedly more intense than the $I(XX)$ one, a result in accordance with the higher density of chromophores expected along the Y direction because of the photoinduced reorientation processes. It is also remarkable that weaker polarization effects are detected in the first case (Figure 8a) leading to relatively large R_1 values varying over the 0.48−0.68 wide range; in contrast, stronger effects take place in the second case (Figure 8b) and weaker R_2 values are found, again nearly equal to 0.33 ± 0.03 (Table 2). This corresponds to a completely new experimental situation, previously never encountered when dealing with several anisotropic samples of uniaxial symmetry.[25,33−35] So, the existence of a biaxial symmetry must be seriously considered and, as demonstrated in the theoretical part, the data treatments imply a careful and simultaneous inspection of both the FTIR and Raman polarization results; this approach is carried out for several vibrational modes in the next discussion section.

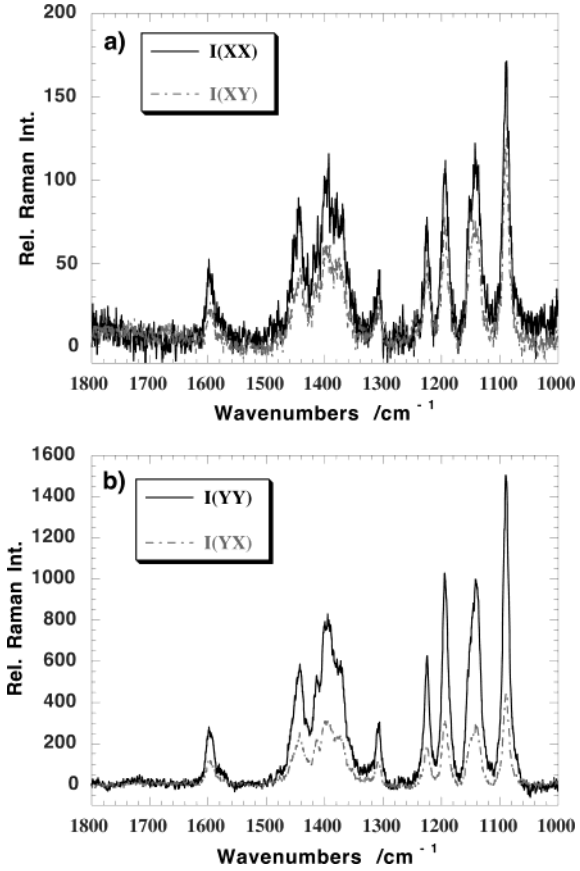

Figure 8. Polarized Raman scattering spectra of a birefringent PAP1−50 thin film in the 1800−1000 cm^{-1} range: (a) the I_{XX} (full lines) and I_{XY} (dashed line) polarized responses; (b) the I_{YY} (full lines) and I_{YX} (dashed line) polarized responses.

Discussion

Under a biaxial model, the f_θ(biax) and f_Φ(biax) factors are easily calculated for several modes using eq 9, and the corresponding values are gathered in Table 1. For the five ring modes located in the 1600−1000 cm^{-1} range, namely ω(C═C) (8a) at 1599 cm^{-1}, (19a) at 1506 cm^{-1}, ν_{asym}(Φ−N) at 1308 cm^{-1}, δ(CH) (9a) at 1141 cm^{-1} and ν_{sym}(Φ−N) at 1089 cm^{-1}, the f_θ(biax) values are still strongly negative with a mean value equal to -0.302 ± 0.017; this confirms that orientation effects are important in the perpendicular directions. In contrast, relatively large and positive values, over the restricted range [+0.341, +0.371] (with an average of $+0.357 \pm 0.012$), are found for the other factor f_Φ(biax) and this demonstrates, for the first time, the existence of an important photoinduced biaxiality in such a grafted azo−polymer system. It is worthwhile to note that slightly different values of f_θ(biax) and f_Φ(biax) are observed for the ν(N═N) vibration at 1372 cm^{-1}, indicating a particular direction of its transition moment (see Table 1). Nevertheless, we may conclude that the long axis of the chromophore units is preferentially oriented along the *Y* axis (in the film plane) than along the *Z* axis (normal to the film). Furthermore, it is also noteworthy that the f_θ(biax) and f_Φ(biax) values of other normal modes of vibration are markedly and differently affected by the anisotropic distribution of the diazo- and azo-mesogen groups; in particular, parallel orientation effects are evidenced on the ν(N−H) band at 3357 cm^{-1}, ν(C═O) mode of ester groups at 1730 cm^{-1}, and ν(C═O) of amide groups at 1676 cm^{-1} since their transition moments are now instead perpendicular to the long molecular axes.

For a comparison purpose, one may recall that the buildup of an optical anisotropy and a photoinduced biaxiality has previously been evidenced by transient absorption experiments and ATR waveguide polarized measurements in a series of K1−*x* photoaddressable copolymers.[5] This suggests that the occurrence of a biaxial symmetry under strong irradiations may be a general property of these absorbing amorphous side-chain polymer systems containing mesogenic and ordinary azo- (or diazo-) benzene moieties; this property was particularly maximized and reinforced in the K1−*x* samples with $x = 30\%$, 40%. Similarly, in the PAP1−50 material under study ($x = 50\%$) the biaxiality appears important, confirming that the cooperative effects play again a great role in the photoinduced alignment processes of the different azobenzene side-chain units.

As emphasized in the theoretical section, we know that the interpretation of the polarized Raman results is not straightforward. However, in connection with the above discussion, we shall concentrate on the Raman data of five common, Infrared and Raman active, modes in the 1600−1000 cm^{-1} region (Table 2). For these vibrations, we already know values of the $\langle \mathbf{F}_{2,0} \rangle$, $\langle \mathbf{F}_{2,2} \rangle$ orientation factors from the infrared analyses and, we first assume a mean value for the next factor, $\langle \mathbf{F}_{4,0} \rangle$. According to the $\langle \mathbf{F}_{2,0} \rangle$ coefficient, the $\langle \mathbf{F}_{4,0} \rangle$ mean value will correspond to the center of the domain of existence for the most probable distribution functions of Gaussian type in the system with a perfect uniaxial symmetry.[20] So, the related quantities vary from +0.054 to +0.103 and they display a relatively large error bar (nearly equal to ±0.032), which corresponds to the broadness of the Gaussian type domain. It is very important to note that the proposed values are in accordance with the fact that any distribution $F(\cos\theta, \Phi)$ must be always positive, whatever the θ and Φ angles are. In fact, under the uniaxial assumption, i.e., according to eq 16 with $\Phi = 45°$ and using $\theta = 0$ or π, the following inequality must apply

$$\langle F_{4,0} \rangle \geq \frac{-1}{9}(5\langle F_{2,0} \rangle + 1) \tag{24}$$

a situation which is entirely satisfied.

Under these conditions, the $\langle \mathbf{F}_{4,2} \rangle$ factor is further readily estimated from the experimental R_1 ratio and the last $\langle \mathbf{F}_{4,4} \rangle$ parameter is calculated from the second experimental R_2 ratio. It must be pointed out that, as expected and underlined by Jarvis et al.,[22] the two following inequalities are fulfilled,

$$|\langle F_{4,2} \rangle| \leq \frac{540}{56} = 9.643 \tag{25}$$

$$|\langle F_{4,4} \rangle| \leq \frac{1680}{16} = 105 \tag{26}$$

and, similarly, the corresponding calculated parameters $\langle \mathbf{P}_{4,j} \rangle$ are also very weak. Indeed, the $\langle \mathbf{P}_{4,2} \rangle$ rough values range from +0.004 to −0.0002, while the $\langle \mathbf{P}_{4,4} \rangle$ ones are varying over the domain −0.009 to −0.054 (Table 2): under these conditions, all the values extracted from the Raman data are physically meaningful. Furthermore, we have checked that error bars as large as 20% in the R_1 and R_2 intensity ratios could give rise to

Table 2. Comparison of Infrared and Raman Results, Values of the Raman Intensity Ratios R_1, R_2 for Several Vibrational Modes, and Estimates of the Main Orientation Factors under the Assumption of a Biaxial Symmetry

	infrared results			Raman results				
mode ν/cm^{-1}	$f_\theta = \langle F_{2,0}\rangle = \langle P_{2,0}\rangle$	f_ϕ	$2f_\phi(1-f_\theta)/\langle F_{2,2}\rangle$ ($\langle P_{2,2}\rangle$)[a]	R_1	R_2	$\langle F_{4,0}\rangle = \langle P_{4,0}\rangle$ (b)	$\langle F_{4,2}\rangle$ ($\langle P_{4,2}\rangle$)[a]	$\langle F_{4,4}\rangle$ ($\langle P_{4,4}\rangle$)[a]
ω(C−C) ring (8a)	−0.304	+0.341	+0.889	0.48	0.30	+0.081	+0.64	−51.65
1599 cm^{-1}			(+0.074)			(±0.033)	(+0.003)	(−0.031)
ν(N═N)	−0.321	+0.243	+0.642	0.58	0.37	+0.097	+0.70	−91.49
1372 cm^{-1}			(+0.053)			(±0.031)	(+0.004)	(−0.054)
ν asym (Φ-N)	−0.295	+0.351	+0.909	0.57	0.37	+0.073	−0. 03	−47.69
1308 cm^{-1}			(+0.076)			(±0.033)	(−0.0002)	(−0.028)
δ(CH) ring (9a)	−0.275	+0.351	+0.895	0.64	0.33	+0.054	−0. 59	−14.68
1141 cm^{-1}			(+0.075)			(±0.033)	(−0.003)	(−0.009)
ν sym (Φ−N)	−0.328	+0.372	+0.986	0.68	0.33	+0.103	−0. 62	−36.58
1089 cm^{-1}			(+0.082)			(±0.030)	(−0.003)	(−0.022)

[a] Value in parentheses of the related $\langle P_{2,2}\rangle$, $\langle P_{4,2}\rangle$, and $\langle P_{4,4}\rangle$ coefficients, respectively. [b] Error bar value in parentheses corresponding to the broadness of related domain of Gaussian type distribution function (see text).

somewhat large variations on the $\langle \mathbf{F}_{4,2}\rangle$ orientation parameter (by a factor of 2.0), but to only very weak changes on the $\langle \mathbf{F}_{4,4}\rangle$ parameter (less than 10%); nevertheless, in all cases the coefficients are still contained within physically suitable domains.

Finally, to get a better insight into the molecular symmetry properties of the copolymer film, it may be useful for the above-discussed vibrational modes to calculate the average squares of the direction cosine of their main transition moment (which lies along the z molecular axis) with respect the *OXYZ* laboratory coordinate system (Figure 2). In agreement with Jarvis et al.,[22] we may use the following equations:

$$\begin{cases} \langle \cos^2(zX)\rangle = \dfrac{1}{3} + \dfrac{2}{3}\langle P_{2,0}\rangle \\ \langle \cos^2(zY)\rangle = \dfrac{1}{3} - \dfrac{1}{3}\langle P_{2,0}\rangle + 2\langle P_{2,2}\rangle \\ \langle \cos^2(zZ)\rangle = \dfrac{1}{3} - \dfrac{1}{3}\langle P_{2,0}\rangle - 2\langle P_{2,2}\rangle \end{cases} \qquad (27)$$

For instance, for the ω(C═C) vibration we calculate ($z\hat{O}X$) = 68.8°, ($z\hat{O}Y$) = 40.3° and ($z\hat{O}Z$) = 57.6°, respectively. Obviously, all these angular values are again in agreement with a biaxial symmetry with a preferential orientation of the chromophores in the film plane.

Finally, to obtain the shape of the corresponding distribution functions we have made use of a mean Φ angle equal to 35.0°, a value in agreement with the average f_ϕ orientation factor equal to 0.342 for the five above-discussed modes. Then, the complete distribution functions are established using proposed values of the orientation coefficients (Table 2) and the analytical expression of eq 16. As an illustrative example, distribution functions in Cartesian and polar coordinates for the ω(C═C) 8a mode are plotted in Figure 9, parts a and b, respectively. This leads to a physically reliable nearly Gaussian-type shape function, which can be nicely distinguished from the distorted function calculated using only the $\langle \mathbf{F}_{2,0}\rangle$ and $\langle \mathbf{F}_{4,0}\rangle$ coefficients and a truncated crude approach. It must be recalled that under the uniaxial approximation different values of both coefficients would be obtained but they would lead to a nonconverging and physically meaningless function. Furthermore, although the reorientation mechanisms in the perpendicular directions are found important and dominant, it is remarkable that the chromophore distribution function is relatively broad with a fwhm roughly equal to 60° (Figure 9a); nevertheless, one notes

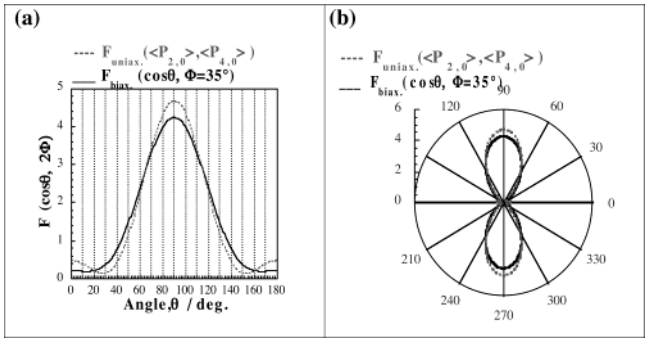

Figure 9. Plots of the final chromophore orientation distribution functions in the birefringent PAP1−50 sample under the biaxial (full line) and uniaxial (dashed line) symmetry assumptions for the ω(C═C) ring mode at 1599 cm^{-1}: (a) in Cartesian coordinates and (b) in a polar representation. Under the uniaxial assumption, the orientation function has been calculated using only the $\langle P_2\rangle$ and $\langle P_4\rangle$ order parameter values, and for a better comparison, the function has been normalized to the same integrated intensity.

for θ values around 0 and 180° (±20°) that the laser beam pumping irradiations were quite efficient, since the distribution nearly vanishes to zero. Actually, the same two functions plotted in polar coordinates look like rather similar but they are distinct in the 0 and 180° regions. Therefore, we do not recommend this representation, which may be confusing and provides (as shown above in Figure 5) a partial view of the symmetry properties in a system. It is thus hard to discriminate between uniaxial and biaxial symmetry and to draw definitive conclusions about the symmetry properties in polymer films from only the inspection of a distribution function in a polar plot representation.

Conclusion

From a complete spectroscopic study we have thus confirmed that strong reorientation photoinduced effects in the PAP1−50 system lead to the establishment of a biaxial symmetry with a preferential orientation of the chromophores in the film plane. From a comparison of the polarized transmission data in UV−visible and infrared regions, we have demonstrated that one may readily conclude the existence of a significant deviation from the uniaxial symmetry. Then, by properly combining infrared results with polarized Raman scattering data, we have been able to propose reliable values for the five orientation factors, $\langle \mathbf{F}_{2,0}\rangle$, $\langle \mathbf{F}_{2,2}\rangle$, $\langle \mathbf{F}_{4,0}\rangle$, $\langle \mathbf{F}_{4,2}\rangle$, and $\langle \mathbf{F}_{4,4}\rangle$, characteristics of a biaxial symmetry property, and to get consistent results about the distribution

orientation functions for several vibrational modes. Furthermore, we have shown that a great care must be applied in the experiments and data treatments, since severe conditions on values of the various orientation factors must be fulfilled.

Furthermore, our proposed method, that we have for the first time extensively developed in the theoretical part, could be applied to further studies of PAP1−50 films under thermal annealing conditions which are known to again increase the birefringence properties; it would be interesting to find a possibility to study this thermal gain-effect in terms of molecular orientation distributions. Results of such studies will be published in due course. Finally, the method could also be extended with success to other homopolymer and copolymer samples, which are known to display large dichroic and birefringent phenomena upon irradiation; these systems are generally treated, only for simplicity, as more simple uniaxial systems.

Acknowledgment. T.B, F.L.L., and C.S. are indebted to the CNRS (Chemistry Department) and to the Région Aquitaine for financial support in FTIR and Raman equipment. They are thankful to Bayer AG for the available polymer films and for a collaboration agreement.

References and Notes

(1) Natansohn, A.; Rochon, P. *Adv. Mater. (Weinheim, Ger.)* **1999**, *11*, 1387.
(2) Natansohn, A.; Rochon, P. *Chem. Rev.* **2002**, *102*, 4139.
(3) Hvilsted, S.; Ramanujam, P. S. *Monatsh. Chem.* **2001**, *132*, 43.
(4) Buffeteau, T.; Pézolet, M. *Macromolecules* **1998**, *31*, 2631.
(5) Cimrova, V.; Neher, D.; Kostromine, S. G.; Bieringer, T. *Macromolecules* **1999**, *32*, 8496.
(6) Dumont, M.; El Osman, A. *Chem. Phys.* **1999**, *245*, 437.
(7) Eich, M.; Wendorff, J. H.; Reck, B.; Ringsdorf, H. *Makromol. Chem. Rapid Commun.* **1987**, *8*, 59.
(8) Hidelbrandt, R.; Hegelich, M.; Keller, H. M.; Marowsky, G.; Hvilsted, S.; N. Holme, C. R.; Ramanujan, P. S. *Phys. Rev. Lett.* **1998**, *81*, 5548.
(9) Pagès, S.; Lagugné Labarthet, F.; Buffeteau, T.; Sourisseau, C. *Appl. Phys. B: Laser Opt.* **2002**, *75*, 541.
(10) Nikolova, L.; Nedelchev, L.; Todorov, T.; Petrova, T.; Tomova, N.; Dragostinova, V.; Ramanujam, P. S.; Hvilsted, S. *Appl. Phys. Lett.* **2000**, *77*, 657.
(11) Nedelchev, L.; Nikolova, L.; Todorov, T.; Petrova, T.; Tomova, N.; Dragostinova, V.; Ramanujam, P. S.; Hvilsted, S. *J. Opt. A: Pure Appl. Opt.* **2001**, *3*, 304.
(12) Wiesner, U.; Reynolds, N.; Boeffel, C.; Spiess, H. W. *Makromol. Chem., Rapid Commun.* **1991**, *12*, 457.
(13) Wiesner, U.; Reynolds, N.; Boeffel, C.; Spiess, H. W. *Liq. Cryst.* **1992**, *11*, 251.
(14) Sabi, Y.; Yamamoto, M.; Watanabe, H.; Bieringer, T.; Haarer, D.; Hagen, R.; Kostromine, S. G.; Berneth, H. *Jpn. J. Appl. Phys.* **2001**, *40*, 1613.
(15) Berneth, H.; Claussen, U.; Kostromine, S. G.; Neigl, R.; Vedder, H.-J. US Patent (Bayer AG, Germany) 6,423,799, 2002, B1, July 23rd, 2002.
(16) Zilker, S. J.; Bieringer, T.; Haarer, D.; Stein, R. S.; VanEgmond, J. W.; Kostromine, S. G. *Adv. Mater.* **1998**, *10*, 855.
(17) Zilker, S. J.; Huber, M. R.; Bieringer, T.; Haarer, D. *Appl. Phys. B: Laser Opt.* **1999**, *68*, 893.
(18) Berne, B. J.; Pechukas, P.; Harp, G. D. *J. Chem. Phys.* **1968**, *49*, 3125.
(19) Pottel, H.; Herreman, W.; Van deer Meer, B. W.; Ameloot, M. *Chem. Phys.* **1986**, *102*, 37.
(20) Lagugné Labarthet, F.; Buffeteau, T.; Sourisseau, C. *Appl. Spectrosc.* **2000**, *54*, 699.
(21) Nomura, S.; Kawai, H.; Kimura, I.; Kagiyama, M. *J. Polym. Sci., Part A-2* **1970**, *8*, 383.
(22) Jarvis, D. A.; Hutchinson, I. J.; Bower, D. I.; Ward, I. M. *Polymer* **1980**, *21*, 41.
(23) Ikeda, R.; Chase, B.; Everall, N. In *Handbook of vibrational spectroscopy*; Chalmers, J. M., Griffiths, P. R., Eds.; John Wiley: Chichester, U.K., 2002; Vol. 1, pp 716−730.
(24) Kaito, A. Nakayama, K.; Kanetsuna, H. L. *Macromol. Sci.—Phys.* **1987**, *B26*, 281.
(25) Lagugné Labarthet, F.; Buffeteau, T.; Sourisseau, C. *J. Phys. Chem. B* **1998**, *102*, 5754.
(26) Lagugné Labarthet, F.; Buffeteau, T.; Sourisseau, C. *Macromol. Symp.* **1999**, *137*, 75.
(27) Turrell, G. *J. Raman Spectrosc.* **1984**, *15*, 103.
(28) Brémard, C.; Laureyns, J.; Merlin, J. C.; Turrell, G. *J. Raman Spectrosc.* **1987**, *18*, 305.
(29) Brémard, C.; Laureyns, J.; Turrell, G. *Can. J. Spectrosc.* **1987**, *32*, 70.
(30) Eickmans, J.; Bieringer, T.; Kostromine, S. G.; Berneth, H.; Thoma, R. *Jpn. J. Appl. Phys., Part 1* **1999**, *38*, 1835.
(31) Bieringer, T.; Kostromine, S. G. Private communication, 2002.
(32) Lagugné Labarthet, F.; Sourisseau, C. *J. Raman Spectrosc.* **1996**, *27*, 491.
(33) Lagugné Labarthet, F.; Buffeteau, T.; Sourisseau, C. *J. Phys. Chem. B* **1999**, *103*, 6690.
(34) Lagugné Labarthet, F.; Bruneel, J. L.; Buffeteau, T.; Sourisseau, C.; Huber, M. R.; Zilker, S. J.; Bieringer, T. *Phys. Chem. Chem. Phys.* **2000**, *2*, 5154.
(35) Lagugné Labarthet, F.; Bruneel, J. L.; Sourisseau, C.; Huber, M. R.; Bôrger, V.; Menzel, H. *J. Raman Spectrosc.* **2001**, *32*, 665.

MA030471G